Method for Estimating Tensiomyography Parameters from Motion Capture Data

Dino Vlahek, Tadej Stošić and Tamara Golob
Institute of Computer Science
Faculty of Electrical Engineering and Computer Science at the University of Maribor, Maribor, Slovenia
E-mail: dino.vlahek1@um.si, tadej.stosic1@um.si, t.golob@um.si

Miloš Kalc, Teja Ličen and Matjaž Vogrin
Institute of Sports Medicine, Faculty of Medicine at the University of Maribor, Maribor, Slovenia
E-mail: milos.kalc@ism-mb.si, teja.licen@um.si, matjaz.vogrin@um.si

Domen Mongus
Institute of Computer Science
Faculty of Electrical Engineering and Computer Science at the University of Maribor, Maribor, Slovenia
E-mail: domen.mongus@um.si

Keywords: tensiomyography, marker-based motion capture, 3D points, geometric transformation

Received: June 05, 2020

Tensiomyography is a muscle performance assessment technique that measures its mechanical responses. In this study, we explored the possibility of replacing traditional tensiomyography measurement systems with motion capture. The proposed method allows the measurement of multiple muscle points simultaneously while achieving measurements during a patient's movements. The results showed that approximately 5 *mm error was achieved when estimating maximal muscle displacement, while time delay in muscle contraction and contraction time was assessed with up to* 20 *ms error. As confirmed by physicians, the introduced errors are within the acceptable margin and, thus, the obtained results are medically valid.*

Povzetek: V članku predstavimo novo metodo, ki omogoča večtočkovno merjenje tensiomiografije. Metoda temelji na snemanju mišične kontrakcije s sistemom za zajem gibanja. Rezultati metode in pripadajoče napake so ovrednoteni s strani zdravnikov. Le-ti ocenjujejo, ali so napake še znotraj sprejemljive meje, da so rezultati medicinsko veljavni.

1 Introduction

Tensiomyography (TMG) is a non-invasive mechanomyography method that measures mechanical muscle response based on radial muscle belly displacement induced by the electrical stimulus. The measurement unit usually includes an electrical stimulator, a data acquisition subunit, a digital sensor, and muscle electrodes [28]. TMG output is a displacement-time curve evaluated with the following parameters: Delay time (T_d) is a time difference between the electrical impulse and 10% of the contraction, contraction time (T_c) is a time difference between 10% and 90% of the contraction, sustain time (T_s) is a time difference between 50% of the contraction and 50% of the relaxation, and relaxation time (T_r) is a time difference between 90% and 50% of the relaxation and maximal displacement of the muscle contraction (D_m).

TMG's resulting parameters are usually used for the evaluation of an individual's maximal speed, explosiveness, endurance, and flexibility [16]. They are also applied in the training optimization process in order to prevent negative effects of muscle asymmetry and asynchrony on an individual's performance [19]. Additionally, after an injury, muscle functional capacity can be assessed using TMG, so that the most effective rehabilitation treatment is administered [21], while its usage in medical research includes estimation of muscle composition [24], evaluation of muscle atrophy [10], measuring adaptation to different pathologies [12], and for determination of muscle fiber type composition [6].

However, TMG has significant drawbacks, as it is a fixed, static tool that can perform single-point measurements [28, 10]. Additionally, the reliability of measurement highly depends on the experiences of the measurer, since placements of sensors and electrodes could affect the reliability of the results [24], while measurements are generally performed in a static and relaxed position [28].

In order to address the above-mentioned drawbacks, we propose a method that generates output similar to TMG using marker-based motion capture. The proposed approach allows for measuring multiple points simultaneously, thus reducing the effort required in order to measure muscle contractions. In addition, the measurements can be achieved not only in the relaxed positions but also while moving, as control markers are used in order to stabilize

natural limb movement in markers. Accordingly, related work in motion capture is described in Section 2. Section 3 introduces a new method that estimates TMG output from motion capture. The proposed method validation results are presented and discussed in Section 4, while section 5 concludes the paper.

2 Related work

Motion capture allows for recording the movement of objects or people. Various motion capturing systems were introduced recently, including acoustical, mechanical, magnetic, and optical ones. The most widely used systems are optical. They use a camera for recording the motions of markers attached to an object [18]. Two types of markers are used for this purpose, namely, passive and active ones. Passive markers reflect light generated by a near camera lens, while the active ones use their own light source. In any case, 3D positions of markers over time can be reconstructed using optical triangulation, and the estimated trajectories can be used for pinpointing positions of displacements for analysis, visualization, and simulation purposes [11]. Both motion capture systems have been used in the entertainment industry for years as well, where its successful implementation ranges from famous films like Avatar and Lord of the rings [1] to the gaming industry [20]. Optical motion tracking usage, with the support of virtual reality, was also demonstrated for tracking and reconstruction of hand movements for sign language interpretation and dance coaching [26]. Furthermore, optical motion capture technology is today an emerging technology in sports and medicine. For instance, its usage was examined for the purposes of facial performance acquisition [13], animation of the natural bending, bulging, and jiggling [4], reconstruction of three-dimensional rotations of human joints [7], and gait analysis [3]. Within this context, the efficiency comparison of marker-less and marker-based motion capture for gait analysis was conducted, where the authors concluded that maker-based motion capture is more suitable for clinical use. A more recent study, however, has shown that motion capture, in general, can introduce errors due to linear scaling and technology imperfection [14]. Here, the musculoskeletal models of different centers of joints, obtained from marker-based motion capture, were scaled and compared with measurements obtained from MRI images that are today believed to be the gold standard.

Nevertheless, optical motion capture is still widely used in sport gesture analysis that ranges from repetitive stresses and movements on the shoulder [23] to underwater body motions [2]. Moreover, efficient utilization of motion capture technology for medical uses was proposed in [22, 25]. In addition, motion capture technology was successfully used for the rehabilitation of patients with spastic hemiplegic cerebral palsy [15] and Duchenne muscular dystrophy [9]. Thus, as marker-based motion capture is frequently used for gait and skeleton analysis in sports medicine and animating 3D objects in the entertainment industry, it provides a solid technological foundation for our study.

3 Method

In this section, a method for estimating TMG parameters from 3D motion capture data is presented. The proposed method uses a set of markers in order to trace muscle contraction using motion capture, while TMG parameters are estimated during the following steps:

- **Point stabilization** is achieved first in order to compensate for natural limb movements and preserve only those movements that result from muscle contractions.
- **Construction of displacement-time curves** is achieved next by estimating displacement distances from stabilized 3D marker positions.
- **Extraction of TMG parameters** is finally achieved based on the estimated displacement-time curve.

Following the description of the mathematical framework, these steps are described in detail.

3.1 Theoretical background

The implementation of the proposed mathematical framework is given in the homogeneous coordinate system. This allows for implementing all the used geometric transformations, including translation, by matrix multiplication and, thus, enables efficient utilization of a graphic processing unit [8].

Let a set of markers $M = \{{}^t m_i\}$, where ${}^t m_i = [{}^t x_i, {}^t y_i, {}^t z_i, 1]$, while i is a markers index and t is the time t of its capture. A vector between points ${}^t m_i$ and ${}^t m_j$ is denoted as ${}^t\vec{v}_{i,j} = {}^t m_i - {}^t m_j$, while its projections to $XY-$ and $XZ-$planes are denoted as ${}^t u_{i,j} = ({}^t x_{i,j}, {}^t y_{i,j}, 1)$ and ${}^t w_i = ({}^t x_{i,j}, {}^t z_{i,j}, 1)$, respectively. A translation for an arbitrary vector ${}^t\vec{v}_{i,j} = ({}^t x_{i,j}, {}^t y_{i,j}, {}^t z_{i,j})$ is then given by a translation matrix M_T, defined as

$$M_T(\vec{v}_T) = \begin{bmatrix} 1 & 0 & 0 & {}^t x_{i,j} \\ 0 & 1 & 0 & {}^t y_{i,j} \\ 0 & 0 & 1 & {}^t z_{i,j} \\ 0 & 0 & 0 & 1 \end{bmatrix}. \tag{1}$$

In addition, rotation matrices $M_{R_y}(\Theta_y)$ and $M_{R_z}(\Theta_z)$ that define rotation around $Y-$ and $Z-$axis for given angles Θ_y and Θ_z, respectively, are denoted by

$$\begin{aligned} M_{R_y}(\Theta_y) &= \begin{bmatrix} cos\Theta_y & 0 & sin\Theta_y & 0 \\ 0 & 1 & 0 & 0 \\ -sin\Theta_y & 0 & cos\Theta_y & 0 \\ 0 & 0 & 0 & 1 \end{bmatrix}, \\ M_{R_z}(\Theta_z) &= \begin{bmatrix} cos\Theta_z & -sin\Theta_z & 0 & 0 \\ sin\Theta_z & cos\Theta_z & 0 & 0 \\ 0 & 0 & 1 & 0 \\ 0 & 0 & 0 & 1 \end{bmatrix} \end{aligned} \tag{2}$$

[27].

3.2 Point stabilization

In order to account for the natural movement of a limb, two control markers were placed on the limb joints in such a way that they were not affected by muscle contractions. They are denoted by the indices $i = 1$ and $i = 2$, while the corresponding vector ${}^t\vec{v}_{1,2}$ was used to stabilize the set of markers M (see Figure 1). In order to achieve stabilization, the origin of coordinate system was shifted to the control marker $i = 1$, while the $X-$axis was aligned with ${}^t\vec{v}_{1,2}$. Note that the latter only requires rotation around $Y-$ and $Z-$axis, while the rotation around $X-$axis can be neglected due to the nature of measurement that limits such limb movements. Thus, rotations around $Y-$ and $Z-$axis were denoted by rotation angles Θ_y and Θ_z, defined as angles between projected vectors ${}^t\vec{u}_{1,2}$ and ${}^t\vec{w}_{1,2}$ and the $X-$axis, respectively [27]. This stabilization, denoted as M_S, is formally defined as

$$M_S = M_T({}^tm_1) \cdot M_{R_y}(\Theta_y) \cdot M_{R_z}(\Theta_z) = \begin{bmatrix} cos^t\Theta_y cos^t\Theta_z & -sin^t\Theta_z cos^t\Theta_y & sin^t\Theta_y & {}^tx_1 \\ sin^t\Theta_z & 0 & 0 & {}^ty_1 \\ -sin^t\Theta_y cos^t\Theta_z & sin^t\Theta_y sin^t\Theta_z & cos^t\Theta_y & {}^tz_1 \\ 0 & 0 & 0 & 1 \end{bmatrix}, \tag{3}$$

where $M_T({}^tm_1)$ denotes translation of the origin of coordinate system to control marker $i = 1$, while $M_{R_y}(\Theta_y)$ and $M_{R_z}(\Theta_z)$ rotations by Θ_y and Θ_z, respectively. Moreover, stabilized set of markers $S = \{{}^ts_i\}$, where ${}^ts_i = ({}^tx'_i, {}^ty'_i, {}^tz'_i)$ is, thus, given as:

$${}^ts_i = M_S \cdot {}^tm_i. \tag{4}$$

3.3 Construction of displacement-time curves and TMG parameters extraction

This step aims to construct a displacement time curves from S and extract the required TMG parameters. As muscle contraction is captured by the movement of stabilized markers, a displacement curve for each marker ${}^ts_i \in S$ is generated by measuring its distance ${}^td_i$ in time $t > 0$ from its starting point, given at $t = 0$. Formally, a displacement curve is given by a discrete mapping function $D : (t, i) \to \mathbb{R}$ defined by:

$$D(t, i) = \sqrt{({}^0s_i - {}^ts_i)^2}. \tag{5}$$

As Eq. 5 cannot produce negative values, it is critical that the initial measurement given at time $t = 0$ is measured in the relaxing (non-contracted) state of the muscle. $D(t, i)$, thus, provides a set of control points based on which a polynomial interpolation is achieved in order to increase the precision of the estimated TMG parameters. As polynomial interpolation is a well-know problem, it is not further discussed here. Its efficient implementation is described in [5]. Moreover, as explained in Section 1, five parameters can be extracted from a displacement curve, where most of the medically relevant information is contained in maximal contraction D_m, delay time T_d, and contraction time T_c. Given an interpolated displacement curve $d_i(t)$, definitions are as follows:

$$\begin{aligned} D_m(i) &= \max_t \ d_i(t), \\ T_d(i) &= \arg\min_t(t; d_i(t) \geq 0.1 \cdot D_m(i)), \\ T_c(i) &= T_d(i) - \arg\min_t(t; d_i(t) \geq 0.9 \cdot D_m(i)). \end{aligned} \tag{6}$$

4 Results and discussion

The proposed method's implementation was done using C++, and experiments were conducted on a workstation with Intel® Core™ i5 CPU and 16 GB of main memory. Experimental data about twelve different participants were collected using a 4×5 matrix of reflective markers that were placed on the quadriceps femoris of participants' left leg, while two control markers were placed over the trochanter head and lateral condyle (see Fig. 1). The participants were instructed to lie supine on a therapeutic table where each placed its left leg on a triangular cushion that provided approximately 30° knee angle support. Then, Rectus Femoris (RF - the upper central part of the thigh) and Vastus Medialis (VM - lower internal part of the thigh) muscles were stimulated with a single electrical impulse provided by a high voltage constant current electrical stimulator, while control measurements were obtained using a traditional TMG sensor (TMG-BMC Ltd, Ljubljana, Slovenia). One series of these measurements consisted of five consecutive muscle stimulation with a 5 s interstimulus intervals in order to prevent post-activation potentiating. For each muscle, six different sets of stimulations were administrated, starting with the stimulation intensity of 30 mA, increasing the power in each measurement by 10 mA, until a maximum of 80 mA was reached. Thus, a total of 30 stimuli for each muscle were measured. At the same time, the same muscle contractions were captured from reflective markers with a Smart-D, BTS s.p.a. motion capture system. The system consisted of eight infrared cameras with 800×600 spatial and 60 Hz temporal resolution, while their position at the therapeutic table is shown in Figure 2.

At each marker, the measured motion capture data was used in order to reconstruct the displacement-time curves, while their agreement with the control TMG curve was estimated in terms of Pearson correlation coefficient [17]. The obtained results are shown in Table 1. Obviously, the displacement-time curves showed a different agreement level with the control TMG measurements, depending on the markers' proximities to the TMG sensor. On average, VM measurements displayed lower correlations with control ones than those performed on RF due to the dilated oscillations of the muscular surface, while those markers

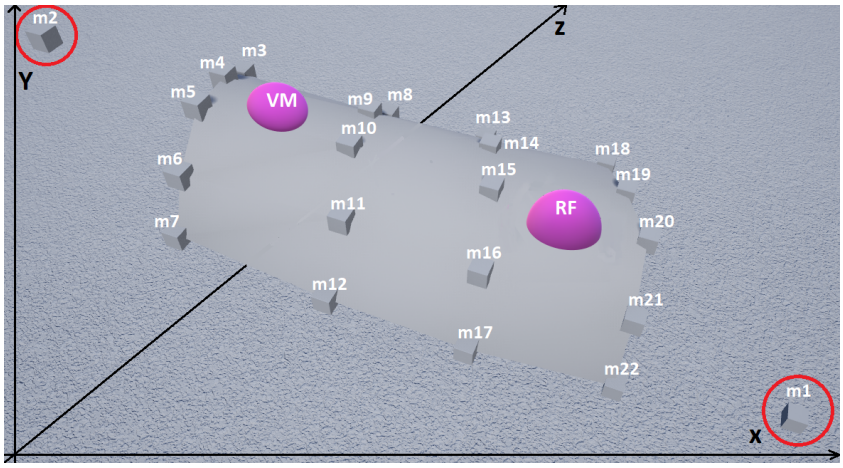

Figure 1: The placement of twenty markers and two control markers on the subject's leg. The Violet area represents the placement of the TMG sensor during measurement, while red circles indicate control markers.

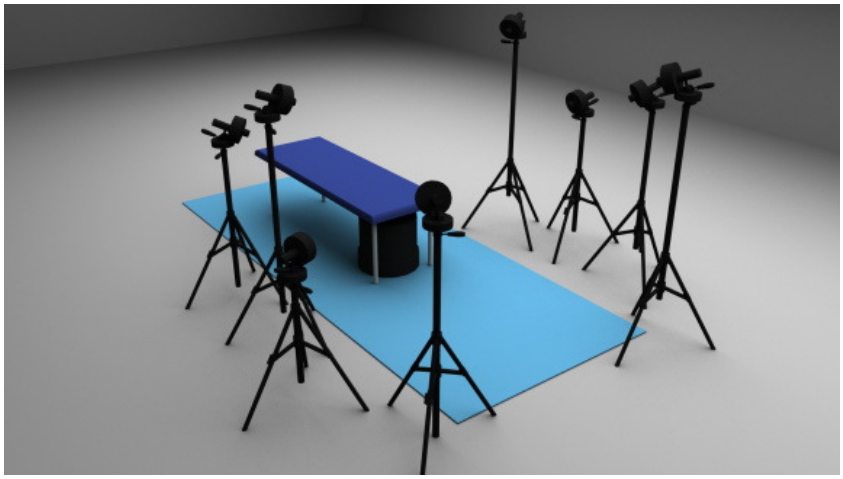

Figure 2: Position of cameras where measurements were performed.

placed near the TMG sensor displayed better correlation in both cases. As follows from Table 1, in the case of VM, the highest correlations with control TMG were measured at $m5$ and $m9$, while $m15$ displayed best results in case of RF stimulation. In addition, the results obtained at $m11$, $m16$, $m19$, and $m20$ were also statistically significant in both cases. Such results are expected as these markers were located in anatomical regions of measured muscles. Displacement-time curves from markers that show the highest agreement with corresponding control TMG curves are further presented in Figure 3, while TMG parameters were extracted from these particular markers and further examined.

In order to assess the accuracy of the extracted TMG parameter, their values were estimated from displacement-time curves generated from markers. Moreover, parameters error rates represent differences between their values and the parameters' values from corresponding control TMG. The results are shown in the appendix (Tables $2-7$). When considering T_c and T_d for VM, the lowest error rates were observed in case of $m5$ at 50 mA and $m20$ at 50 mA with 0.2% and 0%, respectively, while error rates between $1.1-25.3\%$ in case of T_c and $3-30.4\%$ in case T_d were observed in other cases. On the other hand, no error was observed for D_m at $m20$ at 60 mA, while the error rates in other cases ranged between $1.7-61.7\%$. In the case of RF, T_c error rates were in the range of $0.9-33.7\%$, with the smallest related to $m20$ at 30 mA. However, T_d introduced inconsistent error rates, from 1.8% in case of $m16$ at 30 mA, up to 75.7% in case of $m11$ at 60 mA. D_m error rates were between $6.4-33.7\%$, where the lowest one is associated with $m19$ at 80 mA.

According to the evaluation provided by the medical experts, the obtained error rates were within the acceptable ranges and can be considered as medically irrelevant. The error of D_m can be explained by the fact that the TMG sensor is slightly pressed into the soft tissue, resulting in a small depression at a baseline level, causing a higher value of D_m when a traditional TMG is measured. As expected, there were high errors in the T_d parameter since the signals from motion capture and TMG were not properly synchronized. Additionally, obtained errors could be explained by

Table 1: Pearson correlation coefficients between the displacement-time curves of markers and control TMG measurements together with average result according to each marker.

	30 mA		40 mA		50 mA		60 mA		70 mA		80 mA		Average	
	VM	RF	VM	RF	VM	RF	VM	RF	VM	RF	VM	RF	VM	RF
m3	0.652	0.774	0.527	0.803	0.497	0.81	0.514	0.716	0.607	0.701	0.657	0.628	0.575	0.738
m4	0.696	0.745	0.543	0.721	0.504	0.672	0.529	0.557	0.604	0.583	0.698	0.512	0.595	0.632
m5	0.74	0.837	0.606	0.842	0.581	0.839	0.569	0.75	0.637	0.747	0.729	0.672	0.644	0.781
m6	0.604	0.77	0.508	0.76	0.584	0.785	0.538	0.699	0.647	0.732	0.681	0.638	0.594	0.731
m7	0.575	0.735	0.393	0.779	0.352	0.767	0.386	0.677	0.478	0.756	0.515	0.664	0.45	0.73
m8	0.745	0.766	0.578	0.725	0.559	0.686	0.529	0.625	0.63	0.691	0.584	0.644	0.604	0.689
m9	0.73	0.818	0.578	0.825	0.629	0.809	0.621	0.699	0.628	0.723	0.681	0.666	0.644	0.757
m10	0.734	0.732	0.596	0.789	0.578	0.761	0.555	0.767	0.646	0.801	0.718	0.697	0.638	0.757
m11	0.746	0.761	0.573	0.839	0.607	0.845	0.659	0.743	0.652	0.829	0.666	0.644	0.65	0.777
m12	0.531	0.748	0.374	0.796	0.35	0.825	0.365	0.724	0.425	0.79	0.453	0.65	0.417	0.755
m13	0.612	0.738	0.482	0.759	0.431	0.717	0.423	0.656	0.567	0.613	0.55	0.593	0.511	0.679
m14	0.647	0.732	0.525	0.727	0.516	0.668	0.494	0.626	0.605	0.635	0.607	0.654	0.566	0.674
m15	0.729	0.878	0.562	0.846	0.537	0.858	0.6	0.758	0.665	0.81	0.638	0.718	0.622	0.811
m16	0.731	0.789	0.574	0.797	0.589	0.826	0.632	0.724	0.631	0.758	0.669	0.679	0.637	0.762
m17	0.528	0.816	0.45	0.813	0.422	0.801	0.412	0.758	0.408	0.776	0.43	0.693	0.441	0.776
m18	0.567	0.558	0.427	0.603	0.381	0.639	0.406	0.558	0.536	0.535	0.523	0.496	0.473	0.565
m19	0.712	0.795	0.661	0.761	0.62	0.817	0.53	0.714	0.668	0.785	0.647	0.703	0.639	0.763
m20	0.61	0.789	0.632	0.837	0.613	0.819	0.561	0.788	0.698	0.71	0.665	0.691	0.63	0.772
m21	0.641	0.824	0.527	0.796	0.53	0.795	0.484	0.727	0.609	0.761	0.617	0.589	0.563	0.749
m22	0.483	0.76	0.439	0.801	0.542	0.774	0.504	0.688	0.617	0.801	0.576	0.67	0.527	0.749

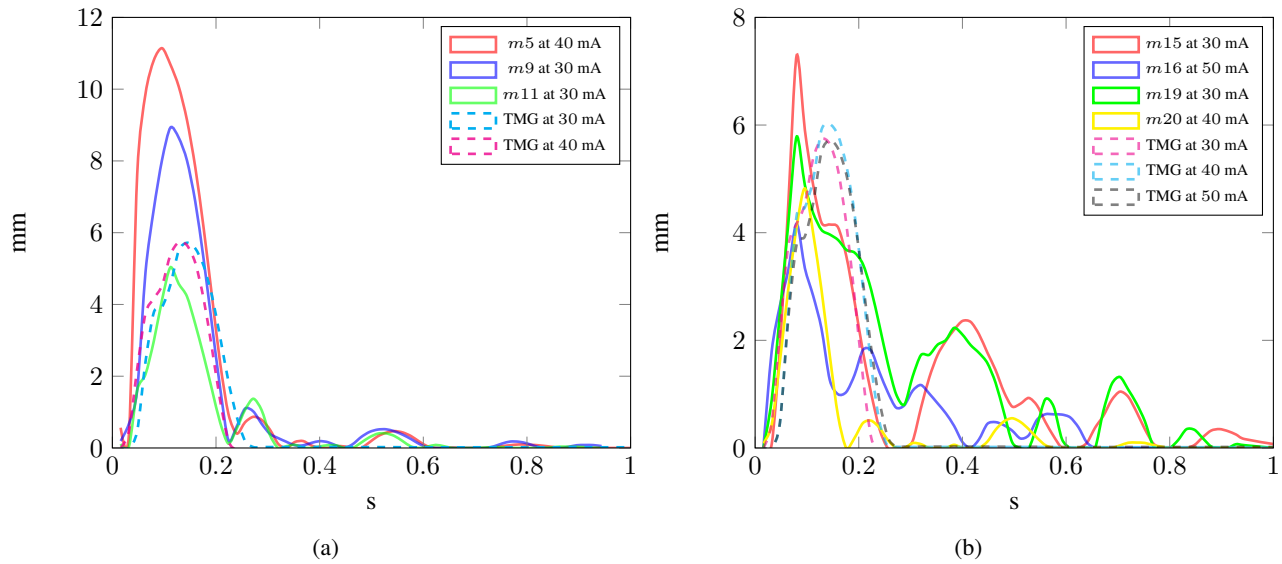

Figure 3: Displacement-time curves from traditional TMG (dashed lines) and corresponding markers (solid lines) that produced the highest level of agreement with traditional TMG for muscle a) VM and b) RF. On the $x-$axis, there is time in s, while the $y-$axis represents displacement in mm.

the fact that the TMG measurement unit provides more precise measurements because of its 1000 Hz temporal resolution when comparing it with 60 Hz of the motion capture system. On the other hand, markers $m19$ and $m11$ registered significant movements, even though they were not placed in the anatomical regions, where contraction of RF and VM was expected. Such an outcome might have different explanations:

- strong electrical stimulation can cause the propagation of the electrical stimuli in deeper tissues, causing muscle contraction of adjacent muscles,
- the passive mass, represented by inactivated muscles and adipose tissue near the stimulated region, can vibrate, causing errors in measurements.

5 Conclusion

A new method for estimating TMG parameters from 3D motion capture, proposed in this paper, allows for measurement of TMG parameters at multiple points simultaneously, while measurements can be obtained during the patient's movement. With the error rates of 5 mm when estimating maximal muscle displacement and up to 20 ms when estimating delay time and contraction time, the provided results proved to be medically relevant. Nevertheless, selection and proper placement of markers are required. One of the future tasks is a synchronization of the TMG and motion capture signals that would allow us to obtain the exact starting time of muscle contraction and, thus, further improved contraction and delay time assessment. In addition, improved point stabilization with compensating for rotations along the X-axis will be considered. Finally, as the described study provides validation of the proposed method from the engineering point of view, the extended medical one is required to prove its real value.

Acknowledgement

This work was supported by the Slovenian Research Agency under Grants J2-8176 and P2-0041, and the project "Wearable Integrated Smart Brace for Rehabilitation Monitoring and Diagnostic of Disorders in Muscular Functions - WIBRANT" that is co-financed by the Republic of Slovenia, Ministry of Education, Science and Sport, and the European Union under the European Regional Development Fund. More info: `www.eu-skladi.si/?set_language=en`.

References

[1] Rufino R. Ansara. and Chris Joslin. Adding cartoon-like motion to realistic animations. In *Proceedings of the 12th International Joint Conference on Computer Vision, Imaging and Computer Graphics Theory and Applications - Volume 1: GRAPP, (VISIGRAPP 2017)*, pages 137–147. INSTICC, SciTePress, 2017. https://doi.org/10.5220/0006174001370147.

[2] Gustavo R. D. Bernardina, Pietro Cerveri, Ricardo M. L. Barros, João C. B. Marins, and Amanda P. Silvatti. Action sport cameras as an instrument to perform a 3d underwater motion analysis. *PLOS ONE*, 11:1–14, 08 2016. https://doi.org/10.1371/journal.pone.0160490.

[3] Elena Ceseracciu, Zimi Sawacha, and Claudio Cobelli. Comparison of markerless and marker-based motion capture technologies through simultaneous data collection during gait: Proof of concept. *PLOS ONE*, 9(3):1–7, 03 2014. https://doi.org/10.1371/journal.pone.0087640.

[4] Caecilia Charbonnier, Frank C. Kolo, Victoria B. Duthon, Nadia Magnenat-Thalmann, Christoph D. Becker, Pierre Hoffmeyer, and Jacques Menetrey. Assessment of congruence and impingement of the hip joint in professional ballet dancers: A motion capture study. *The American Journal of Sports Medicine*, 39(3):557–566, 2011. https://doi.org/10.1177/0363546510386002.

[5] M. F. I. Chowdhury, C. Jeannerod, V. Neiger, E. Schost, and G. Villard. Faster algorithms for multivariate interpolation with multiplicities and simultaneous polynomial approximations. *IEEE Transactions on Information Theory*, 61(5):2370–2387, May 2015. https://doi.org/10.1109/TIT.2015.2416068.

[6] Raja Dahmane, Srdjan Djordjevic, Bostjan Simunic, and Vojko Valencic. Spatial fiber type distribution in normal human muscle Histochemical and tensiomyographical evaluation. *Journal of biomechanics*, 38(12):2451–2459, 2005. https://doi.org/10.1016/j.jbiomech.2004.10.020.

[7] R. Degeorges, J. Parasie, D. Mitton, N. Imbert, J.-N. Goubier, and F. Lavaste. Three-dimensional rotations of human three-joint fingers: an optoelectronic measurement. preliminary results. *Surgical and Radiologic Anatomy*, 27(1):43–50, Mar 2005. https://doi.org/10.1007/s00276-004-0277-4.

[8] Peng Du, Rick Weber, Piotr Luszczek, Stanimire Tomov, Gregory Peterson, and Jack Dongarra. From CUDA to OpenCL: Towards a performance-portable solution for multi-platform GPU programming. *Parallel Computing*, 38(8):391 – 407, 2012. https://doi.org/10.1016/j.parco.2011.10.002.

[9] Raluca Ganea, Pierre-Yves Jeannet, A. Paraschiv-Ionescu, Nathalie Goemans, Christine Piot, Marleen Hauwe, and Kamiar Aminian. Gait assessment in children with duchenne muscular dystrophy during long-distance walking. *Journal of child neurology*, 27:30–8, 07 2011. https://doi.org/10.1177/0883073811413581.

[10] Oscar Garcia-Garcia, Alba Cuba-Dorado, Tania Alvarez-Yates, Javier Carballo-Lopez, and Mario Iglesias-Caamano. Clinical utility of tensiomyography for muscle function analysis in athletes. *Open Access Journal of Sports Medicine*, 10:49–69, 2019. https://doi.org/10.2147/OAJSM.S161485.

[11] Michael Gleicher. Animation from observation: Motion capture and motion editing. *SIGGRAPH Comput. Graph.*, 33(4):51–54, November 1999. https://doi.org/10.1145/345370.345409.

[12] K. Grabljevec, H. Burger, K. Kersevan, V. Valencic, and C. Marincek. Strength and endurance of knee extensors in subjects after paralytic poliomyelitis.

Disability and Rehabilitation, 27(14):791–799, July 2005. https://doi.org/10.1080/09638280400020623.

[13] Haoda Huang, Jinxiang Chai, Xin Tong, and Hsiang-Tao Wu. Leveraging motion capture and 3D scanning for high-fidelity facial performance acquisition. *ACM Trans. Graph.*, 30(4):74:1–74:10, July 2011. https://doi.org/10.1145/2010324.1964969.

[14] Hans Kainz, Hoa Hoang, Chris Stockton, Roslyn Boyd, David Lloyd, and Christopher Carty. Accuracy and reliability of marker based approaches to scale the pelvis, thigh and shank segments in musculoskeletal models. *Journal of Applied Biomechanics*, 33:1–21, 03 2017. https://doi.org/10.1123/jab.2016-0282.

[15] M.C.M. Klotz, L. Kost, F. Braatz, V. Ewerbeck, D. Heitzmann, S. Gantz, T. Dreher, and S.I. Wolf. Motion capture of the upper extremity during activities of daily living in patients with spastic hemiplegic cerebral palsy. *Gait & Posture*, 38(1):148–152, 2013. https://doi.org/10.1016/j.gaitpost.2012.11.005.

[16] Irineu Loturco, Saulo Gil, Cristiano Laurino, Hamilton Roschel, Ronaldo Kobal, Cesar Abad, and Fabio Nakamura. Differences in muscle mechanical properties between elite power and endurance athletes: A comparative study. *The Journal of Strength and Conditioning Research*, 29(6):1723–1728, 12 2014. https://doi.org/10.1519/JSC.0000000000000803.

[17] J. Neyman and E. S. Pearson. On the problem of the most efficient tests of statistical hypotheses. *Philosophical Transactions of the Royal Society of London. Series A, Containing Papers of a Mathematical or Physical Character*, 231:289–337, 1933. https://doi.org/10.1098/rsta.1933.0009.

[18] Haldun M. Ozaktas and Levent Onural. *Three-Dimensional Television: Capture, Transmission, Display*. Springer Science & Business Media, 2007. https://doi.org/10.1007/978-3-540-72532-9.

[19] Ezequiel Rey, Carlos Lago-Penas, and Joaquin Lago-Ballesteros. Tensiomyography of selected lower-limb muscles in professional soccer players. *Journal of Electromyography and Kinesiology*, 22(6):866 – 872, 2012. https://doi.org/10.1016/j.jelekin.2012.06.003.

[20] A. L. Rincon, H. Yamasaki, and S. Shimoda. Design of a video game for rehabilitation using motion capture, emg analysis and virtual reality. In *2016 International Conference on Electronics, Communications and Computers (CONIELECOMP)*, pages 198–204, Feb 2016. https://doi.org/10.1109/CONIELECOMP.2016.7438575.

[21] Pedro S Dias, Joan S Fort, Daniel A Marinho, Albano Santos, and MÃąrio Marques. Tensiomyography in physical rehabilitation of high level athletes. *The Open Sports Sciences Journal*, 3:47–48, 03 2014. https://doi.org/10.2174/1875399X010030100047.

[22] L. A. Schwarz, A. Mkhitaryan, D. Mateus, and N. Navab. Estimating human 3D pose from time-of-flight images based on geodesic distances and optical flow. In *Face and Gesture 2011*, pages 700–706, 2011. https://doi.org/10.1109/FG.2011.5771333.

[23] Elena Seminati, Alessandra Marzari, Oreste Vacondio, and Alberto Minetti. Shoulder 3D range of motion and humerus rotation in two volleyball spike techniques: injury prevention and performance. *Sports Biomechanics*, 14(2):216–231, 07 2015. https://doi.org/10.1080/14763141.2015.1052747.

[24] Bostjan Simunic. Between-day reliability of a method for non-invasive estimation of muscle composition. *Journal of electromyography and kinesiology*, 22:527–30, 04 2012. https://doi.org/10.1016/j.jelekin.2012.04.003.

[25] Ivo Stancic, Tamara Grujic Supuk, and Ante Panjkota. Design, development and evaluation of optical motion-tracking system based on active white light markers. *IET Science, Measurement & Technology*, 7:206–214(8), July 2013. https://doi.org/10.1049/iet-smt.2012.0157.

[26] Jeff Tang, J.C.P. Chan, and H. Leung. Interactive dancing game with real-time recognition of continuous dance moves from 3D human motion capture. *5th International Conference on Ubiquitous Information Management and Communication*, pages 50–58, 01 2011. https://doi.org/10.1145/1968613.1968674.

[27] John Vince. *Mathematics for Computer Graphics*. Springer-Verlag, Berlin, Heidelberg, 5th edition, 2014. https://doi.org/10.1007/978-1-4471-7336-6.

[28] T. Zagar and D. Krizaj. Validation of an accelerometer for determination of muscle belly radial displacement. *Medical and Biological Engineering and Computing*, 43(1):78–84, February 2005. https://doi.org/10.1007/BF02345126.

6 Appendix

Table 2: The table shows average values and associated standard deviation for parameters extracted from markers at a stimulation intensity of 30 mA. Associated errors were placed below the results. The lowest errors are highlighted.

	Vastus medialis			Rectus femoris		
	$T_c\ (ms)$	$T_d\ (ms)$	$D_m\ (mm)$	$T_c\ (ms)$	$T_d\ (ms)$	$D_m\ (mm)$
m5	39 (± 15.95)	27.2 (± 11.43)	6.5 (± 3.58)	47.2 (± 7.14)	36.7 (± 8.21)	3.4 (± 1.16)
m9	41.8 (± 17.95)	19.4 (± 3.23)	9 (± 5.08)	55.1 (± 7.56)	28.3 (± 9.84)	3 (± 1.43)
m11	43.5 (± 19.18)	21.6 (± 5.48)	5.3 (± 3.31)	59.2 (± 15.13)	27.6 (± 11.02)	2.9 (± 1.8)
m15	44.8 (± 20.08)	21.9 (± 4.64)	7.4 (± 4.74)	49.4 (± 6.01)	33.8 (± 6.75)	4.9 (± 1.8)
m16	45.3 (± 17.85)	22 (± 4.47)	5.2 (± 3.28)	50.5 (± 10.46)	26.1 (± 10.68)	3.5 (± 1.11)
m19	45.7 (± 18.22)	25.4 (± 9.35)	5 (± 3.62)	50.4 (± 6.9)	34.8 (± 11.04)	2.8 (± 1.35)
m20	41.9 (± 17.6)	29.1 (± 10.43)	4.8 (± 3.42)	51 (± 4.5)	29.8 (± 7.58)	3.3 (± 1.33)
TMG	36.5 (± 14.11)	24.2 (± 2.93)	4.9 (± 1.31)	51.5 (± 20.1)	25.6 (± 3.37)	4.3 (± 1.4)
	$Error(T_c)$	$Error(T_d)$	$Error(D_m)$	$Error(T_c)$	$Error(T_d)$	$Error(D_m)$
m5	**2.5** (6.9 %)	**3.0** (12.4 %)	**1.6** (33.7%)	4.3 (8.4%)	11.1 (43.2%)	0.9 (20.4%)
m9	5.4 (14.7 %)	4.8 (19.8 %)	4.1 (83.7%)	3.6 (6.9%)	2.7 (10.4%)	1.3 (30.9%)
m11	7.1 (19.4 %)	2.6 (10.8 %)	0.4 (8.7%)	7.7 (14.9%)	2.0 (8.0%)	1.5 (33.8%)
m15	8.3 (22.9 %)	2.3 (9.3 %)	2.5 (51.1%)	2.1 (4.1%)	8.2 (32.2%)	0.5 (12.5%)
m16	8.8 (24.2 %)	2.2 (9.0 %)	0.3 (6.8%)	**1.0** (1.9%)	**0.5** (1.8%)	**0.8** (18.8%)
m19	9.2 (25.3 %)	1.2 (5.0 %)	0.2 (3.2%)	1.1 (2.2%)	9.2 (36.0%)	1.5 (33.8%)
m20	5.4 (14.9 %)	4.9 (20.4 %)	0.1 (1.9%)	0.5 (0.9%)	4.2 (16.4%)	1.0 (22.9%)

Table 3: The table shows average values and associated standard deviation for parameters extracted from markers at a stimulation intensity of 40 mA. Associated errors were placed below the results. The lowest errors are highlighted.

	Vastus medialis			Rectus femoris		
	$T_c\ (ms)$	$T_d\ (ms)$	$D_m\ (mm)$	$T_c\ (ms)$	$T_d\ (ms)$	$D_m\ (mm)$
m5	30.9 (± 11.9)	29.1 (± 16.9)	6.9 (± 3.7)	47 (± 10.8)	35.4 (± 13.7)	4 (± 1)
m9	33.1 (± 14.5)	24 (± 14.1)	6.9 (± 5.6)	50.9 (± 7.8)	33.7 (± 10.6)	3.8 (± 1.7)
m11	35.3 (± 16)	24.8 (± 12.7)	5.5 (± 2.6)	55.3 (± 14.5)	30.3 (± 9.9)	3.8 (± 2.1)
m15	33.6 (± 15.1)	26.2 (± 13.7)	7.8 (± 4.7)	50.2 (± 7.3)	33.9 (± 7.2)	6.2 (± 1.7)
m16	36.2 (± 14)	25.9 (± 13.8)	5.3 (± 3)	54.3 (± 10)	29.1 (± 10.1)	4.3 (± 2)
m19	35.3 (± 13.4)	28.7 (± 15.5)	5.4 (± 4.1)	49.3 (± 6.1)	34.9 (± 10.8)	3.2 (± 0.8)
m20	35.6 (± 12.5)	28 (± 13.8)	5.1 (± 3.8)	49.9 (± 6.8)	32 (± 11)	4.3 (± 1.4)
TMG	31.3 (± 10.9)	23.1 (± 2.5)	5.7 (± 1.8)	45.1 (± 18.3)	24.8 (± 3.1)	4.9 (± 1.6)
	$Error(T_c)$	$Error(T_d)$	$Error(D_m)$	$Error(T_c)$	$Error(T_d)$	$Error(D_m)$
m5	0.3 (1.1 %)	6 (25.8 %)	1.2 (20.3%)	1.9 (4.2%)	10.7 (43%)	0.9 (18.2%)
m9	**1.8** (5.7 %)	**0.9** (3.8 %)	**1.2** (21.0%)	5.8 (12.9%)	8.9 (36%)	1 (21.4%)
m11	4.1 (13 %)	1.6 (7.1 %)	0.2 (3.5%)	10.2 (22.7%)	5.5 (22.3%)	1.1 (21.7%)
m15	2.3 (7.4 %)	3.1 (13.2 %)	2.1 (36.3%)	5.1 (11.3%)	9.1 (36.9%)	1.3 (26.9%)
m16	4.9 (15.8 %)	2.8 (12.1 %)	0.4 (6.2%)	**9.2** (20.5%)	**4.3** (17.6%)	**0.6** (11.8%)
m19	4 (12.8 %)	5.6 (24.1 %)	0.4 (6.2%)	4.2 (9.4%)	10.1 (40.8%)	1.6 (33.9%)
m20	4.3 (13.7 %)	4.8 (20.9 %)	0.6 (10.8%)	4.9 (10.8%)	7.2 (29.3%)	0.6 (11.9%)

Table 4: The table shows average values and associated standard deviation for parameters extracted from markers at a stimulation intensity of 50 mA. Associated errors were placed below the results. The lowest errors are highlighted.

	Vastus medialis			Rectus femoris		
	$T_c\ (ms)$	$T_d\ (ms)$	$D_m\ (mm)$	$T_c\ (ms)$	$T_d\ (ms)$	$D_m\ (mm)$
m5	28.93 (± 11.01)	23.89 (± 8.60)	7.35 (± 3.76)	48.14 (± 4.01)	38.70 (± 13.90)	12.86 (± 1.29)
m9	31.41 (± 12.99)	19.56 (± 4.33)	10.07 (± 5.65)	49.42 (± 4.20)	39.29 (± 16.25)	6.19 (± 2.01)
m11	33.45 (± 15.45)	19.91 (± 3.23)	6.62 (± 2.65)	46.98 (± 4.67)	39.21 (± 17.36)	9.83 (± 1.75)
m15	30.44 (± 14.53)	20.99 (± 5.26)	9.08 (± 4.76)	50.57 (± 6.98)	36.57 (± 9.64)	8.00 (± 1.73)
m16	33.12 (± 14.47)	21.45 (± 6.30)	6.50 (± 2.92)	48.79 (± 4.89)	39.78 (± 13.43)	4.56 (± 1.72)
m19	31.90 (± 13.95)	23.77 (± 8.49)	6.14 (± 4.32)	49.07 (± 3.34)	37.13 (± 11.97)	4.31 (± 0.78)
m20	31.93 (± 14.84)	23.11 (± 7.21)	6.09 (± 3.83)	53.01 (± 4.79)	29.9 (± 11.49)	9.15 (± 1.21)
TMG	28.86 (± 9.14)	23.08 (± 2.24)	6.31 (± 1.88)	42.04 (± 5.22)	24.44 (± 2.98)	18.97 (± 1.66)
	$Error(T_c)$	$Error(T_d)$	$Error(D_m)$	$Error(T_c)$	$Error(T_d)$	$Error(D_m)$
m5	**0.1** (0.2 %)	**0.8** (3.5 %)	**1.0** (16.5%)	6.1 (14.5%)	14.3 (58.3%)	1.2 (23.1%)
m9	2.5 (8.8 %)	3.5 (15.3 %)	3.8 (59.5%)	7.4 (17.6%)	14.8 (60.5%)	1.0 (19.5%)
m11	4.6 (15.9 %)	3.2 (13.7 %)	0.3 (4.8%)	4.9 (11.8%)	14.8 (60.5%)	0.6 (10.6%)
m15	1.6 (5.5 %)	2.1 (9.0 %)	2.8 (43.9%)	8.5 (20.3%)	12.1 (49.6%)	1.8 (33.6%)
m16	4.3 (14.7 %)	1.6 (7.0 %)	0.2 (3.0%)	6.7 (16.0%)	15.3 (62.7%)	0.3 (6.4%)
m19	3.0 (10.5 %)	0.7 (3.0 %)	0.2 (3.0%)	7.0 (16.7%)	12.7 (51.9%)	1.9 (36.0%)
m20	3.1 (10.6 %)	0.0 (0.0 %)	0.2 (3.0%)	**11.0** (26.1%)	**5.5** (22.5%)	**0.4** (8.3%)

Table 5: The table shows average values and associated standard deviation for parameters extracted from markers at a stimulation intensity of 60 mA. Associated errors were placed below the results. The lowest errors are highlighted.

	Vastus medialis			Rectus femoris		
	$T_c\ (ms)$	$T_d\ (ms)$	$D_m\ (mm)$	$T_c\ (ms)$	$T_d\ (ms)$	$D_m\ (mm)$
m5	29.5 (± 9)	25.4 (± 10.5)	7.6 (± 3.8)	47.3 (± 13.2)	35.2 (± 10.9)	4 (± 1.7)
m9	30.2 (± 12.2)	21.6 (± 8.9)	10.8 (± 5.6)	45.7 (± 4.3)	39 (± 19.2)	4.5 (± 2.4)
m11	32.8 (± 12.3)	20.7 (± 5.3)	7.6 (± 2.9)	40.9 (± 10.4)	43 (± 24.3)	5 (± 2.4)
m15	31.1 (± 14.1)	22 (± 7.1)	10.3 (± 4.8)	51.1 (± 11.7)	32 (± 6.4)	7.3 (± 3)
m16	33.6 (± 15.6)	22.8 (± 8.6)	7.5 (± 3)	45.1 (± 3)	38.8 (± 17.5)	5.1 (± 2.4)
m19	32.8 (± 13.4)	25 (± 10)	6.8 (± 4.3)	46.7 (± 4.9)	38.1 (± 18)	3.4 (± 1.3)
m20	32.8 (± 13.2)	25 (± 9.5)	7 (± 3.8)	51 (± 9)	31.9 (± 10.6)	4.7 (± 1.7)
TMG	28.2 (± 9.2)	23 (± 2.1)	6.9 (± 1.7)	41.5 (± 19.4)	24.5 (± 2.8)	5.7 (± 1.9)
	$Error(T_c)$	$Error(T_d)$	$Error(D_m)$	$Error(T_c)$	$Error(T_d)$	$Error(D_m)$
m5	**1.3** (4.7 %)	**2.4** (10.4 %)	**0.6** (9.1%)	5.8 (13.9%)	10.8 (44.1%)	1.7 (29.3%)
m9	2.1 (7.4 %)	1.4 (6.2 %)	3.9 (55.8%)	4.1 (10%)	14.6 (59.5%)	1.2 (21.4%)
m11	4.6 (16.5 %)	2.3 (9.8 %)	0.7 (10%)	0.6 (1.4%)	18.5 (75.7%)	0.7 (11.8%)
m15	3 (10.5 %)	1 (4.5 %)	3.3 (48.2%)	9.6 (23%)	7.5 (30.7%)	1.6 (27.7%)
m16	5.4 (19.2 %)	0.2 (0.9 %)	0.6 (8.2%)	3.6 (8.6%)	14.4 (58.8%)	0.6 (10.8%)
m19	4.7 (16.6 %)	2 (8.8 %)	0.1 (1.7%)	5.2 (12.4%)	13.6 (55.8%)	2.3 (41%)
m20	4.7 (16.6 %)	1.9 (8.4 %)	0 (0.0%)	**9.5** (22.8%)	**7.5** (30.6%)	**1** (17.3%)

Table 6: The table shows average values and associated standard deviation for parameters extracted from markers at a stimulation intensity of 70 mA. Associated errors were placed below the results. The lowest errors are highlighted.

	Vastus medialis			Rectus femoris		
	$T_c\ (ms)$	$T_d\ (ms)$	$D_m\ (mm)$	$T_c\ (ms)$	$T_d\ (ms)$	$D_m\ (mm)$
m5	31.3 (± 11.7)	26.5 (± 24.9)	8 (± 3.7)	50.3 (± 19.2)	23.2 (± 7.1)	4.5 (± 1.4)
m9	37.6 (± 23.8)	21.4 (± 6.6)	12 (± 5.2)	51.3 (± 10.1)	25.9 (± 6.5)	5.3 (± 1.8)
m11	38.1 (± 23.7)	22 (± 7.5)	8.4 (± 2.7)	45.2 (± 5.6)	33.8 (± 12.8)	5.6 (± 1.9)
m15	33.3 (± 16.8)	26.1 (± 17.3)	11.4 (± 4.4)	46.1 (± 5.4)	31.8 (± 9.1)	8.4 (± 2)
m16	39.8 (± 24)	22.6 (± 8.5)	8.3 (± 2.8)	45.5 (± 3.1)	32.8 (± 13.1)	5.9 (± 1.7)
m19	34.8 (± 14.1)	30 (± 23.2)	7.6 (± 4.2)	53 (± 8.3)	23.3 (± 3.3)	3.9 (± 0.9)
m20	34.5 (± 12)	30.4 (± 25.3)	7.6 (± 3.6)	46.8 (± 3.4)	27.2 (± 8.5)	5.9 (± 1)
TMG	32 (± 19.5)	23.3 (± 2.7)	7.4 (± 2)	48.2 (± 24.4)	24.7 (± 3.1)	6.4 (± 2.3)
	$Error(T_c)$	$Error(T_d)$	$Error(D_m)$	$Error(T_c)$	$Error(T_d)$	$Error(D_m)$
m5	**0.7** (2.2 %)	**3.2** (13.7 %)	**0.6** (7.7%)	2.1 (4.4%)	1.5 (6.1%)	1.9 (30.2%)
m9	5.6 (17.5 %)	2 (8.5 %)	4.6 (61.7%)	3.1 (6.4%)	1.2 (4.7%)	1.1 (16.5%)
m11	6.1 (19.1 %)	1.3 (5.8 %)	1 (13.6%)	3 (6.1%)	9 (36.5%)	0.8 (12.7%)
m15	1.3 (3.9 %)	2.8 (11.9 %)	4 (53.3%)	2.1 (4.3%)	7 (28.4%)	2 (30.9%)
m16	7.8 (24.4 %)	0.8 (3.2 %)	0.9 (11.5%)	2.8 (5.7%)	8.1 (32.6%)	0.5 (7.4%)
m19	2.8 (8.6 %)	6.7 (28.6 %)	0.1 (1.7%)	4.8 (9.9%)	1.4 (5.8%)	2.5 (39.2%)
m20	2.5 (7.7 %)	7.1 (30.4 %)	0.2 (2.6%)	**1.4** (3%)	**2.5** (10%)	**0.5** (7.5%)

Table 7: The table shows average values and associated standard deviation for parameters extracted from markers at a stimulation intensity of 80 mA. Associated errors were placed below the results. The lowest errors are highlighted.

	Vastus medialis			Rectus femoris		
	$T_c\ (ms)$	$T_d\ (ms)$	$D_m\ (mm)$	$T_c\ (ms)$	$T_d\ (ms)$	$D_m\ (mm)$
m5	26.8 (± 7.6)	21.1 (± 13.3)	8.5 (± 3.4)	39.4 (± 12.7)	20.9 (± 10.0)	4.1 (± 1.3)
m9	29.7 (± 15.3)	15.2 (± 1.7)	13.1 (± 4.6)	36.8 (± 9.4)	25.2 (± 12.7)	5.7 (± 1.4)
m11	32.8 (± 17.2)	15.8 (± 2.3)	9.3 (± 2.3)	35.2 (± 9.1)	24.4 (± 13.2)	4.8 (± 1.8)
m15	29.0 (± 14.0)	17.6 (± 6.2)	12.5 (± 3.8)	31.3 (± 9.4)	31.4 (± 11.8)	7.1 (± 2.4)
m16	32.2 (± 18.4)	16.2 (± 2.9)	9.2 (± 2.5)	31.5 (± 4.5)	31.5 (± 13.5)	4.9 (± 1.3)
m19	30.3 (± 10.7)	20.1 (± 10.9)	8.1 (± 4.0)	35.2 (± 7.7)	25.1 (± 14.6)	3.4 (± 1.3)
m20	28.5 (± 10.9)	20.5 (± 11.7)	8.3 (± 3.3)	33.9 (± 5.8)	26.1 (± 13.5)	5.2 (± 1.1)
TMG	31.4 (± 19.5)	23.8 (± 3.6)	7.6 (± 2.3)	47.6 (± 24.3)	24.8 (± 3.3)	6.7 (± 2.7)
	$Error(T_c)$	$Error(T_d)$	$Error(D_m)$	$Error(T_c)$	$Error(T_d)$	$Error(D_m)$
m5	4.6 (14.6 %)	2.7 (11.3 %)	0.9 (11.7%)	8.2 (17.1%)	3.9 (15.6%)	2.6 (39.1%)
m9	1.7 (5.4 %)	8.6 (36 %)	5.4 (71%)	**10.7** (22.6%)	**0.4** (1.6%)	**1** (15.0%)
m11	1.4 (4.5 %)	8 (33.8 %)	1.7 (22%)	12.4 (26.1%)	0.4 (1.6%)	1.9 (28.8%)
m15	2.4 (7.7 %)	6.2 (26.1 %)	4.9 (64.1%)	16.2 (34.1%)	6.6 (26.8%)	0.5 (7.1%)
m16	0.8 (2.4 %)	7.6 (32.1 %)	1.6 (20.9%)	16 (33.7%)	6.7 (27.1%)	1.8 (26.7%)
m19	**1.1** (3.5 %)	**3.7** (15.5 %)	**0.5** (6.4%)	2.4 (26%)	0.3 (1.4%)	3.3 (48.8%)
m20	2.9 (9.2 %)	3.3 (14 %)	0.6 (8.2%)	13.6 (28.6%)	1.3 (5.2%)	1.4 (21.4%)